The Topological Structure of Scale-Space Images

Luc Florack Arjan Kuijper

Abstract

We investigate the "deep structure" of a scale-space image. The emphasis is on topology, *i.e.* we concentrate on critical points—points with vanishing gradient—and top-points—critical points with degenerate Hessian—and monitor their displacements, respectively generic morsifications in scale-space. Relevant parts of catastrophe theory in the context of the scale-space paradigm are briefly reviewed, and subsequently rewritten into coordinate independent form. This enables one to implement topological descriptors using a conveniently defined, global coordinate system.

1 Introduction

1.1 Historical Background

A fairly well understood way to endow an image with a topology is to embed it into a one-parameter family of images known as a "scale-space image". The parameter encodes "scale" or "resolution" (coarse/fine scale means low/high resolution, respectively).

Among the simplest is the linear or Gaussian scale-space model. Proposed by Iijima [13] in the context of pattern recognition it went largely unnoticed for a couple of decades, at least outside the Japanese scientific community. Another early Japanese contribution is due to Otsu [32]. The Japanese accounts are quite elegant and can still be regarded up-to-date in their way of motivating Gaussian scale-space; for a translation, the reader is referred to Weickert, Ishikawa, and Imiya [41]. The earliest accounts in the English literature are due to Witkin [42] and Koenderink [18]. Koenderink's account is particularly instructive for the fact that the argumentation is based on a precise notion of *causality* (in the resolution domain), which allows one to interpret the process of blurring as a well-defined generalisation principle akin to similar ones used in cartography, and also for the fact that it pertains to *topological structure*.

1.2 Scale and Topology

The quintessence is that *scale provides topology*. In fact, by virtue of the scale degree of freedom one obtains a hierarchy of topologies enabling transitions between coarse and fine scale descriptions. This is often exploited in coarse-to-fine algorithms for detecting and localising relevant features (edges, corners, segments, *etc.*).

The core problem—the embodiment of a decent topology—had already been addressed by the mathematical community well before practical considerations in signal and image analysis boosted the development of scale-space theory. Of particular interest is the *theory of tempered distributions* formulated by Laurent Schwartz in the early fifties [34]. Indeed, the mere postulate of *positivity* imposed on the admissible test functions proposed by Schwartz, together with a *consistency requirement*[1] suffices to

[1]The consistency requirement, the details of which are stated elsewhere [5, 6], imposes a convolution-algebraic structure on admissible filter classes in the linear case at hand. Both Schwartz' "smooth functions of rapid decay" as well as Koenderink's Gaussian family are admissible. The autoconvolution algebra generated by the normalised zeroth order Gaussian scale-space filter is unique in Schwartz space given the constraint of positivity.

single out Gaussian scale-space theory from the theory of Schwartz. Moreover, straightforward application of distribution theory readily produces the complete Gaussian family of derivative filters as proposed by Koenderink in the framework of front-end visual processing [24]. For details on Schwartz' theory and its connection to scale-space theory *cf.* the monograph by Florack [6]. In view of ample literature on the subject we will henceforth assume familiarity with the basics of Gaussian scale-space theory [6, 12, 29, 35].

1.3 Deep Structure

In their original accounts both Koenderink as well as Witkin proposed to investigate the "deep structure" of an image, *i.e. structure at all levels of resolution simultaneously*. Today, the handling of deep structure is still an outstanding problem in applications of scale-space theory. Nevertheless, many heuristic approaches have been developed for specific purposes that do appear promising. These typically utilise some form of scale selection and/or linking scheme, *cf.* Bergholm's edge focusing scheme [2], Lindeberg's feature detection method [29, 30], the scale optimisation criterion used by Niessen *et al.* [31] and Florack *et al.* [9] for motion extraction, Vincken's hyperstack segmentation algorithm [40], *etc.*. Encouraged by the results in specific image analysis applications an increasing interest has recently emerged trying to establish a generic underpinning of deep structure. Results from this could serve as a common basis for a diversity of multiresolution schemes. Such bottom-up approaches invariably rely on *catastrophe theory*.

1.4 Catastrophe Theory

An early systematic account of catastrophe theory is due to Thom [37, 38], although the interested reader will probably prefer Poston and Stewart's [33] or Arnold's account [1] instead. Koenderink has pointed out that a scale-space image defines a *versal family*, to which Thom's classification theorem can be applied [10, 33, 37, 38]. "Versal" means that almost all members are generic (*i.e.* "typical" in a precise sense). However, although this is something one could reasonably expect, it is *not* self-evident. On the one hand, the situation is simplified by virtue of the existence of only one control parameter: isotropic inner scale. On the other hand, there is a complication, *viz.* the fact that scale-space is constrained by a p.d.e.[2]: the *isotropic diffusion equation*. The control parameter at hand is special in the sense that it is in fact the evolution parameter of this p.d.e.

Catastrophe theory in the context of the scale-space paradigm is now fairly well-established. It has been studied, among others, by Damon [4]—probably the most comprehensive account on the subject—as well as by Griffin [11], Johansen [14, 15, 16], Lindeberg [27, 28, 29], and Koenderink [19, 20, 21, 22, 25]. An algorithmic approach has been described by Tingleff [39]. Closely related to the present article is the work by Kalitzin [17], who pursues a nonperturbative topological approach.

1.5 Canonical versus Covariant Formalism

The purpose of the present article is twofold: (i) to collect relevant results from the literature on catastrophe theory, and (ii) to express these in terms of user-defined coordinates. More specifically we derive covariant expressions for the tangents to the critical curves in scale-space, both through Morse as well as non-Morse critical points (or top-points[3]), establish a covariant interpolation scheme for the locations

[2] p.d.e. = "partial differential equation".

[3] The term "top-point" is somewhat misleading; we will use it to denote *any* point in scale-space where critical points merge or separate.

of the latter in scale-space, and compute the curvature of the critical curves at the top-points, again in covariant form.

The requirement of covariance is a novel and important aspect not covered in the literature. It entails that one abstains—from the outset—from any definite choice of coordinates. The reason for this is that in practice one is not given the special, so-called "canonical coordinates" in terms of which catastrophe theory is invariably formulated in the literature. Canonical coordinates are chosen to look nice on paper, and as such greatly contribute to our understanding, but in the absence of an operational definition they are of little practical use. A covariant formalism—by definition—allows us to use whatever coordinate convention whatsoever. All computations can be carried out in a global, user-defined coordinate system, say a Cartesian coordinate system aligned with the grid of the digital image.

2 Theory

Theory is presented as follows. First we outline the general plan of catastrophe theory (Section 2.1), and then consider it in the context of scale-space theory (Section 2.2). An in-depth analysis is presented in subsequent sections in canonical (Section 2.3), respectively arbitrary coordinate systems (Section 2.4). The first three sections mainly serve as a review of known facts scattered in the literature, and more or less suffice if the sole purpose is to gain insight in deep structure. The remainder covers novel aspects that are useful for exploiting this insight in practice, *i.e.* for coding deep structure given an input image.

2.1 The Gist of Catastrophe Theory

A critical point of a function is a point at which the gradient vanishes. Typically this occurs at isolated points where the Hessian has nonzero eigenvalues. The *Morse Lemma* states that the qualitative properties of a function at these so-called *Morse critical points* are essentially determined by the quadratic part of the Taylor series (the *Morse canonical form*).

However, in many practical situations one encounters *families* of functions that depend on *control parameters*. An example of a control parameter is scale in a scale-space image. Catastrophe theory is the study of how the critical points change as the control parameters change.

While varying a control parameter in a continuous fashion, a Morse critical point will move along a *critical curve*. At isolated points on such a curve one of the eigenvalues of the Hessian may become zero, so that the Morse critical point turns into a *non-Morse critical point*. Having several control parameters to play with one can get into a situation in which ℓ eigenvalues of the Hessian vanish simultaneously, leaving $n-\ell$ of them nonzero. The *Thom Splitting Lemma* simplifies things: It states that, in order to study the degeneracies, one can simply discard the $n-\ell$ "nice" variables corresponding to the regular $(n-\ell)\times(n-\ell)$-submatrix of the Hessian, and thus study only the ℓ "bad" ones [37, 38]. That is, one can split up the function into a Morse and a non-Morse part, and study the canonical forms of each in isolation, because the same splitting result holds in a full neighbourhood of a non-Morse function. Again, the Morse part can be canonically described in terms of the quadratic part of the Taylor series. The non-Morse part can also be put into canonical form, called the *catastrophe germ*, which is a polynomial of order 3 or higher.

The Morse part does not change qualitatively after a small perturbation. Critical points may move and corresponding function values may change, but nothing will happen to their type: if i eigenvalues of the Hessian are negative prior to perturbation (a "Morse i-saddle"), then this will still be the case afterwards. Thus—from a topological point of view—there is no need to scrutinise the perturbations.

The non-Morse part, on the other hand, does change qualitatively upon perturbation. In general, the non-Morse critical point of the catastrophe germ will split into a number of Morse critical points.

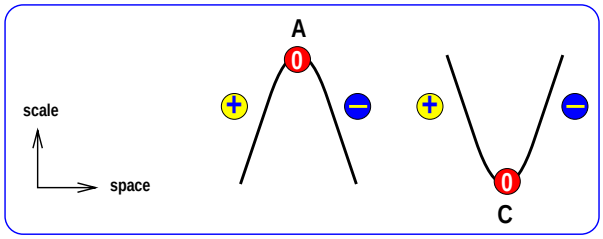

Figure 1: The generic catastrophes in isotropic scale-space. Left: annihilation of a pair of Morse critical points. Right: creation of a pair of Morse critical points. In both cases the points involved have opposite Hessian signature. In 1D, positive signature signifies a minimum, while a negative one indicates a maximum; creation is prohibited by the diffusion equation. In multidimensional spaces creations do occur generically, but are typically not as frequent as annihilations.

This state of events is called *morsification*. The Morse saddle types of the isolated Morse critical points involved in this process are characteristic for the catastrophe. *Thom's Theorem* provides an exhaustive list of "elementary catastrophes" ($1, \ldots, 5$ control parameters), with canonical formulas for the catastrophe germs as well as for the perturbations needed to describe their morsification [37, 38].

2.2 Catastrophe Theory and the Scale-Space Paradigm

One should not carelessly transfer Thom's results to scale-space, since there is a nontrivial constraint to be satisfied: Any scale-space image, together with all admissible perturbations, must satisfy the *isotropic diffusion equation*. Damon has shown how to extend the theory in this case in a systematic way [4].

That Damon's account is somewhat complex is mainly due to his aim for completeness and rigour. If we restrict our attention to *generic* situations only, and consider only "typical" input images that are not subject to special conditions such as symmetries, things are actually fairly simple. The only generic morsifications in scale-space are *creations* and *annihilations* of pairs of Morse hypersaddles of opposite Hessian signature[4]: Fig. 1 (for a proof, see Damon [4]). Everything else can be expressed as a compound of isolated events of either of these two types (although one may not always be able to segregate the elementary events due to numerical limitations).

In order to facilitate the description of topological events, Damon's account, following the usual line of approach in the literature, relies on a slick choice of coordinates. However, these so-called "canonical coordinates" are inconvenient in practice, unless one provides an operational scheme relating them to user-defined coordinates. Mathematical accounts fail to be operational in the sense that—in typical cases—canonical coordinates are at best proven to exist. Their mathematical construction often relies on manipulations of the physically void trailing terms of a Taylor series expansion, in other words, on derivatives up to infinite order, and consequently lacks an operational counterpart. Even if one were in the possession of an algorithm one should realize that canonical coordinates are in fact *local* coordinates. Each potential catastrophe in scale-space would thus require an independent construction of a canonical frame.

The line of approach that exploits suitably chosen coordinates is known as the *canonical formalism*. It provides the most parsimonious way to approach topology if neither metrical relations nor numerical computations are of interest. Thus its role is primarily to *understand* topology. In the next section we give a self-contained summary of the canonical formalism for the generic cases of interest.

[4] "Hessian signature" means "sign of the Hessian determinant evaluated at the location of the critical point".

2.3 Canonical Formalism

The two critical points involved in a creation or annihilation event always have opposite Hessian signature (this will be seen below), so that this signature may serve to define a conserved "topological charge" intrinsic to these critical points. It is clear (by definition!) that the charge of Morse-critical points can never change, as this would require a zero-crossing of the Hessian determinant, violating the Morse criterion that all Hessian eigenvalues should be nonzero. Thus the interesting events are the interactions of charges within a neighbourhood of a non-Morse critical point.

Definition 1 (Topological Charge) *A Morse-critical point is assigned a topological charge $q = \pm 1$ corresponding to the sign of the Hessian determinant evaluated at that point. A regular point has zero topological charge. The topological charge of a non-Morse critical point equals the sum of charges of all Morse-critical points involved in the morsification.*

In anticipation of the canonical coordinate convention, in which the first variable is identified to be the "bad" one, and in which also a second somewhat special direction shows up, it is useful to introduce the following notation.

Notation 1 *We henceforth adhere to the following coordinate conventions:*

$$\mathbf{x} \stackrel{\text{def}}{=} (x_1, \ldots, x_n) \in \mathbb{R}^n \quad , \quad \mathbf{y} \stackrel{\text{def}}{=} (x_2, \ldots, x_n) \in \mathbb{R}^{n-1} \, .$$

Instead of x_1 and x_2 we shall write x and y, respectively.

This notation will allow us to account for signals and images of different dimensions (typically $n = 1, 2, 3$) within a single theoretical framework.

Definition 2 (Catastrophe Germs) *Using Notation 1 we define the catastrophe germs*

$$g^{\text{A}}(x;t) \stackrel{\text{def}}{=} x^3 + 6xt \quad , \quad g^{\text{C}}(x,y;t) \stackrel{\text{def}}{=} x^3 - 6x(y^2 + t) \, ,$$

together with their perturbations

$$f^{\text{A}}(\mathbf{x};t) \stackrel{\text{def}}{=} g^{\text{A}}(x;t) + Q(\mathbf{y};t) \quad , \quad f^{\text{C}}(\mathbf{x};t) \stackrel{\text{def}}{=} g^{\text{C}}(x,y;t) + Q(\mathbf{y};t) \, .$$

The quadric $Q(\mathbf{y};t)$ is defined as follows:

$$Q(\mathbf{y};t) \stackrel{\text{def}}{=} \sum_{k=2}^{n} \epsilon_k \, \left(x_k^2 + 2t \right) \, ,$$

in which each ϵ_k is either $+1$ or -1.

Note that germs as well as perturbations satisfy the diffusion equation

$$\frac{\partial u}{\partial t} = \Delta u \, . \tag{1}$$

In the canonical formalism it is conjectured that, given a generic event in scale-space, one can always set up coordinates in such a way that qualitative behaviour is summarised by one of the two "canonical forms" given above. Note that, even though it does describe the effect of a general perturbation in a *full* scale-space neighbourhood of the catastrophe, the quadric actually does not depend on x. At the location of the catastrophe exactly one Hessian eigenvalue vanishes. The forms $f^{\text{A}}(\mathbf{x};t)$ and $f^{\text{C}}(\mathbf{x};t)$

correspond to an annihilation and a creation event at the origin, respectively (*v.i.*). The latter requires $n \geq 2$; creations will not be observed in 1D signals.

Both events are referred to as "fold catastrophes". The diffusion equation imposes a constraint that manifests itself in the asymmetry of these two canonical forms. In fact, whereas the annihilation event is relatively straightforward, a subtlety can be observed in the creation event, *viz.* the fact that the possibility for creations to occur requires space to be at least two-dimensional[5]. The asymmetry of the two generic events reflects the one-way nature of blurring; topology tends to simplify as scale increases, albeit not monotonically.

2.3.1 The A-Germ

Morsification of the A-germ of Definition 2 entails an annihilation of two critical points of opposite charge as resolution is diminished.

Result 1 (Morsification of the A-Germ) *Recall Definition 2. For $t < 0$ we have two Morse-critical points carrying opposite charge, for $t > 0$ there are none. At $t = 0$ the two critical points collide and annihilate. The critical curves are parametrised as follows:*

$$\mathbf{P}_{\pm} : (x, \mathbf{y}; t)_{\pm} = (\pm\sqrt{-2t}, \mathbf{0}; t)\,.$$

See Fig. 2. It follows from the parametrisation that the critical points collide with infinite opposite velocities before they disappear. Thus one must be cautious and take the parametrisation into account if one aims to link corresponding critical points near annihilation.

Annihilations of the kind described by Result 1 are truly "one-dimensional" events. At the origin both branches of critical curves are tangential to the (x, t)-plane, and in fact approach eachother from opposite spatial directions tangential to $t = 0$, and—in this canonical case—perpendicular to the Hessian zero-crossing[6]. In numerical computations one must account for the fact that near annihilation corresponding critical points are separated by a distance of the order $\mathcal{O}(\sqrt{\Delta t})$ if Δt is the "time[7]-to-collision".

For 1D signals this summarises the analysis of generic events in scale-space. For images there are other possibilities, which are studied below. In 2D images the present case describes the annihilation of a minimum or maximum with a saddle. Minima cannot annihilate maxima, nor can saddles annihilate eachother. In 3D images one has two distinct types of hypersaddles, one with a positive and one with a negative topological charge. Also minima and maxima have opposite charges in this case, and so there are various possibilities for annihilation all consistent with charge conservation. However, charge conservation is only a constraint and does not permit one to conclude that all events consistent with it will actually occur. In fact, by continuity and genericity one easily appreciates that a Morse i-saddle can only interact with a $(i-1)$-saddle ($i = 1, \ldots, n$), because one and only one Hessian eigenvalue is likely to change sign when traversing the top-point (*i.e.* the degenerate critical point) along the critical path. Genericity implies that sufficiently small perturbations will not affect the annihilation event qualitatively. It may undergo a small dislocation in scale-space, but it is bound to occur.

[5] The germ $f^{\mathrm{C}}(\mathbf{x}; t)$ seems to capture *another catastrophe* happening at a somewhat coarser scale some distance away from the origin, yet invariably coupled to the creation event. However, it should be stressed that canonical forms like these are not intended to describe events away from the origin. Indeed, the associated "scatter" event turns out to be highly nongeneric, and is therefore of little practical interest.

[6] "Hessian zero-crossing" is shorthand for "zero-crossing of the Hessian determinant".

[7] "Time" in the sense of the evolution parameter of Eq. (1).

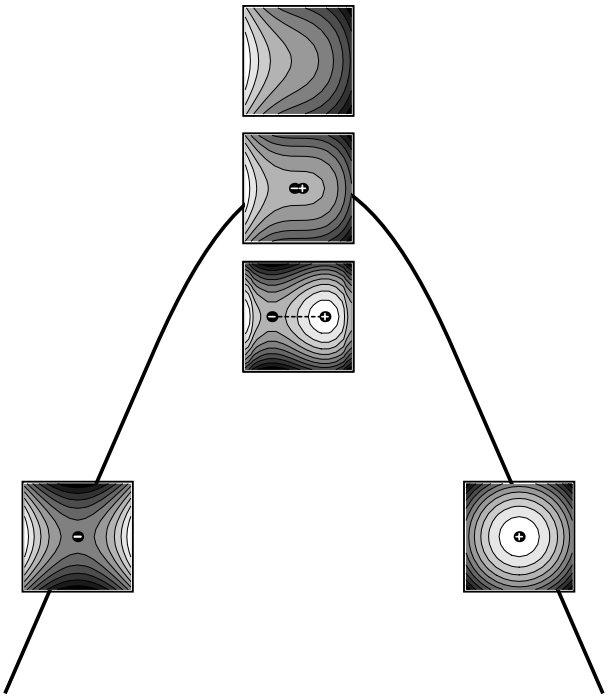

Figure 2: In 2D, positive Hessian determinant signifies an extremum, while a negative one indicates a saddle. The morsification is visualised here for the annihilation event (Result 1), showing five typical, fixed-scale local pictures at different points on or near the critical curve.

2.3.2 The C-Germ

Morsification of the C-germ of Definition 2 entails a creation of two critical points of opposite charge as resolution is diminished. (For a while there has been some confusion about this in the literature; creation events were—falsely—believed to violate the causality principle that is the core of scale-space theory [18].) The event of interest here is the one occurring in the immediate vicinity of the origin.

Result 2 (Morsification of the C-Germ) *Recall Definition 2. For $t < 0$ there are no Morse-critical points in the immediate neighbourhood of the origin. At $t = 0$ two critical points of opposite charge emerge producing two critical curves for $t > 0$. The critical curves are parametrised as follows:*

$$\mathbf{P}_{\pm} : (x, \mathbf{y}; t)_{\pm} = (\pm\sqrt{2t}, \mathbf{0}; t)\,.$$

Again charges are conserved, and again the emerging critical points escape their point of creation with infinite opposite velocities. Genericity implies that creations will persist despite perturbations, and will suffer at most a small displacement in scale-space.

2.3.3 The Canonical Formalism: Summary

To summarize, creation and annihilation events together complete the list of possible generic catastrophes. The canonical formalism enables a fairly simple description of what can happen topologically. However, canonical coordinates do not coincide with user-defined coordinates, and cease to be useful if one aims to compute metrical properties of critical curves. This limitation led us to develop the covariant formalism, which is presented in the next section.

2.4 Covariant Formalism

In practice the separation into "bad" and "nice" coordinate directions is not given. The actual realization of canonical coordinates varies from point to point, a fact that might lead one to believe that it requires an expensive procedure to handle catastrophes in scale-space. However, the covariant formalism declines from the explicit construction of canonical coordinates altogether. It allows us (i) to carry out computations in any *user-defined, global coordinate system*, requiring only a few image convolutions per level of scale, and (ii) to compute *metrical properties* of topological events (angles, directions, velocities, accelerations, *etc.*).

The covariant formalism relies on tensor calculus. The only tensors we shall need are (i) metric tensor $g_{\mu\nu}$ and its dual $g^{\mu\nu}$ (the components of which equal the Kronecker symbol δ^{μ}_{ν} in a Cartesian frame, *i.e.* 1 if $\mu = \nu$, otherwise 0), (ii) Levi-Civita tensor $\varepsilon_{\mu_1 \dots \mu_n}$ and its dual $\varepsilon^{\mu_1 \dots \mu_n}$ in n dimensional space, and (iii) covariant image derivatives (equal to partial derivatives in a Cartesian frame). In a Cartesian frame the Levi-Civita tensor is defined as the completely antisymmetric tensor with $\varepsilon_{1,\dots,n} = 1$; from this any other nontrivial component follows from permuting indices and toggling signs. Actually, we will only encounter products containing an even number of Levi-Civita tensors, which can always be rewritten in terms of metric tensors only (see *e.g.* Florack *et al.* [7] for details). Wherever possible we will use matrix notation to alleviate theoretical difficulties so that familiarity with the tensor formalism is not necessary.

Derivatives are computed by linear filtering:

$$L_{\mu_1 \dots \mu_k} \stackrel{\text{def}}{=} (-1)^k \int dz\, f(z)\, \phi_{\mu_1 \dots \mu_k}(z)\,. \tag{2}$$

Here, $(-1)^k \phi_{\mu_1 \dots \mu_k}(z)$ is the k-th order transposed covariant derivative of the normalised Gaussian $\phi(z)$ with respect to $z^{\mu_1}, \dots, z^{\mu_k}$, tuned to the location and scale of interest (these parameters have been left out for notational simplicity), and $f(z)$ represents the raw image. In particular, the components of the image gradient and Hessian are denoted by L_μ and $L_{\mu\nu}$, respectively. Instead of "covariant derivative" one can read "partial derivative" as long as one sticks to Cartesian frames or rectilinear coordinates. (This is all we need below.) Distributional differentiation according to Eq. (2) is *well-posed* because it is actually integration. Well-posedness admits discretisation and quantisation of Eq. (2), and guarantees that other sources of small scale noise are not fatal. Of course the filters need to be realistic; for scale-space filters this means that one keeps their scales confined to a physically meaningful interval, and that one keeps their differential order below an appropriate upper bound [3]. Equally important is the observation that Eq. (2) makes differentiation operationally *well-defined*. One can actually extract derivatives from an image in the first place, because things are arranged in such a way that, unlike with "classical" differentiation and corresponding numerical differencing schemes, *differentiation precedes discrete sampling*. In practice one will almost always calculate derivatives at all points in the image domain; in that case Eq. (2) is replaced by a *convolution* of f and $\phi_{\mu_1 \dots \mu_k}$ (the minus sign is then implicit).

The ensemble of image derivatives up to k-th order provides a model of local image structure in a full scale-space neighbourhood, known as the *local jet of order* k [8, 10, 23, 24, 26, 33]. Here it suffices to consider structure up to fourth order at the voxel[8] of interest (summation convention applies):

$$\begin{aligned} \overset{(4)}{L}(\mathbf{x}; t) \;=\; & L + L_\mu\, x^\mu + \frac{1}{2} L_{\mu\nu}\, x^\mu x^\nu + \Delta L\, t + \frac{1}{6} L_{\mu\nu\rho}\, x^\mu x^\nu x^\rho + \Delta L_\mu\, x^\mu t + \\ & + \frac{1}{24} L_{\mu\nu\rho\sigma}\, x^\mu x^\nu x^\rho x^\sigma + \frac{1}{2} \Delta L_{\mu\nu}\, x^\mu x^\nu t + \frac{1}{2} \Delta^2 L\, t^2\,. \end{aligned} \tag{3}$$

[8]The term "voxel" refers to a "pixel" in arbitrary dimensions.

The $n+1$ constraints for a non-Morse critical point are

$$\left\{\begin{array}{rcl} \nabla \overset{(4)}{L}(\mathbf{x};t) & = & 0\,, \\ \det \nabla\nabla^{\mathrm{T}} \overset{(4)}{L}(\mathbf{x};t) & = & 0\,, \end{array}\right. \tag{4}$$

which become generic in $(n+1)$-dimensional scale-space. For a Morse critical point one simply omits the determinant constraint, leaving n equations in n unknowns (and 1 scale parameter).

Let us investigate the system of Eqs. (3–4) in the immediate vicinity of a critical point of interest. Assume that $(\mathbf{x};t) = (\mathbf{0};0)$ labels a fiducial grid point near the desired zero-crossing, which has been designated as the base point for the numerical coefficients of Eq. (3). Both gradient as well as Hessian determinant at the corresponding (or any neighbouring) voxel will be small, though odds are that they are not exactly zero. Then we know that Eq. (4) will be solved for $(\mathbf{x};t) \approx (\mathbf{0};0)$, and we may use perturbation theory for interpolation to establish a lowest order sub-voxel solution.

The details are as follows. Introduce a formal parameter $\varepsilon \approx 0$ corresponding to the order of magnitude of the left hand sides of Eq. (4) at the fiducial origin. Substitute $(\mathbf{x};t) = \varepsilon\,(\mathbf{x}_1;t_1)$ into Eq. (4) and collect terms of order $\mathcal{O}(\varepsilon)$ (the terms of order zero vanish by construction). Absorbing the formal parameter back into the scaled quantities the result is the following linear system:

$$\left\{\begin{array}{rcll} L_{\mu\nu}\,x^\nu + \Delta L_\mu\,t & = & -L_\mu & (\mu = 1,\ldots,n)\,, \\ \widetilde{L}^{\mu\nu} L_{\mu\nu\rho}\,x^\rho + \widetilde{L}^{\mu\nu}\Delta L_{\mu\nu}\,t & = & -\|L_{\mu\nu}\|\,, & \end{array}\right. \tag{5}$$

in which the $\widetilde{L}^{\mu\nu}$ are the components of the transposed cofactor matrix obtained from the Hessian (Appendix A), and $\|L_{\mu\nu}\|$ denotes the Hessian determinant[9]. The determinant constraint (last identity) follows from a basic result in perturbation theory for matrices:

$$\det(\mathbf{A} + \varepsilon\,\mathbf{B}) = \det\mathbf{A} + \varepsilon\,\mathrm{tr}\,(\widetilde{\mathbf{A}}\mathbf{B}) + \mathcal{O}(\varepsilon^2)\,. \tag{6}$$

In Eq. (5) both the coefficients on the left hand side as well as the data on the right hand side can be obtained by staightforward linear filtering of the raw image as defined by Eq. (2), so that we indeed have an operationally defined interpolation scheme for locating critical points within the scale-space continuum. It is important to note that the system of Eq. (5) holds *in any coordinate system* (manifest covariance). We will exploit this property in our algorithmic approach later on.

Our next goal is to invert the system of Eq. (5) *while maintaining manifest covariance*. This obviates the need for numerical inversions or the construction of canonical frames. Such methods would have to be applied to each and every candidate voxel in scale-space, while neither would give us much insight in local critical curve geometry. The inversion differs qualitatively for Morse and non-Morse critical points and so we consider the two cases separately.

It is convenient to rewrite Eq. (5) in matrix form with the help of the definitions

$$\mathbf{H}_{\mu\nu} \overset{\mathrm{def}}{=} L_{\mu\nu}\,, \tag{7}$$

$$\mathbf{w}_\mu \overset{\mathrm{def}}{=} \Delta L_\mu\,, \tag{8}$$

$$\mathbf{z}_\mu \overset{\mathrm{def}}{=} L_{\mu\nu\rho}\widetilde{L}^{\nu\rho}\,, \tag{9}$$

$$\mathbf{g}_\mu \overset{\mathrm{def}}{=} L_\mu\,, \tag{10}$$

$$\mathrm{c} \overset{\mathrm{def}}{=} \Delta L_{\mu\nu}\widetilde{L}^{\mu\nu}\,. \tag{11}$$

[9]This abuse of notation—there are actually *no* free indices in $\|L_{\mu\nu}\|$—is common in classical tensor calculus.

Note that

$$\begin{aligned} \mathbf{H} &= \nabla \mathbf{g} \,, && (12) \\ \mathbf{w} &= \partial_t \mathbf{g} \,, && (13) \\ \mathbf{z} &= \nabla \det \mathbf{H} \,, && (14) \\ \mathrm{c} &= \partial_t \det \mathbf{H} \,, && (15) \end{aligned}$$

so that we may conclude that all relevant information is contained in first order spatial and scale derivatives of the image's gradient and Hessian determinant.

With this notation $(n+1) \times (n+1)$ coefficient matrix of Eq. (5) becomes

$$\mathrm{M} \stackrel{\mathrm{def}}{=} \begin{bmatrix} \mathbf{H} & \mathbf{w} \\ \mathbf{z}^{\mathrm{T}} & \mathrm{c} \end{bmatrix} . \tag{16}$$

For Morse critical points at fixed resolution the relevant subsystem in the hyperplane $t = 0$ is

$$\mathbf{H}\mathbf{x} = -\mathbf{g} \,, \tag{17}$$

but in fact we obtain a linear approximation of the *critical curve* through the Morse critical point of interest if we allow scale to vary:

$$\mathbf{H}\mathbf{x} = -\left(\mathbf{g} + \mathbf{w}\, t\right) . \tag{18}$$

This can be easily generalised to any desired order. For top-points we must consider the full system

$$\mathrm{M} \begin{bmatrix} \mathbf{x} \\ t \end{bmatrix} = - \begin{bmatrix} \mathbf{g} \\ \det \mathbf{H} \end{bmatrix} . \tag{19}$$

2.4.1 Morse Critical Points

From Eq. (18) it follows that at level $t = 0$ the tangent to the critical path in scale-space is given by

$$\begin{bmatrix} \mathbf{x} \\ t \end{bmatrix} = \begin{bmatrix} \mathbf{x}_0 \\ 0 \end{bmatrix} + \begin{bmatrix} \mathbf{v} \\ c \end{bmatrix} t \tag{20}$$

in which the sub-voxel location of the Morse critical point is given by

$$\mathbf{x}_0 = -\mathbf{H}^{\mathrm{inv}} \mathbf{g} \,, \tag{21}$$

and its instantaneous scale-space velocity—*i.e.* the displacement in scale-space per unit of t—by

$$\begin{bmatrix} \mathbf{v} \\ 1 \end{bmatrix} = \begin{bmatrix} -\mathbf{H}^{\mathrm{inv}} \mathbf{w} \\ 1 \end{bmatrix} . \tag{22}$$

Note that the path followed by Morse critical points is always transversal to the hyperplane $t = 0$, which is why we can set the scale component equal to unity. In other words, such critical points can never vanish "just like that"; they necessarily have to change identity into a non-Morse variety. According to Eq. (22), spatial velocity $\mathbf{v}$ becomes infinite as the point moves towards a degeneracy (odds are that $\mathbf{w}$ remains nonzero). If we do not identify "time" with scale, but instead reparametrise $t = \det \mathbf{H}\, \tau$, then scale-space velocity—now defined as the displacement per unit of τ—becomes

$$\begin{bmatrix} \mathbf{v}' \\ \mathrm{c}' \end{bmatrix} = \begin{bmatrix} -\widetilde{\mathbf{H}} \mathbf{w} \\ \det \mathbf{H} \end{bmatrix} . \tag{23}$$

With this refinement of the scale parameter the singularity is approached "horizontally" from a spatial direction perpendicular to the null-space of the Hessian (note, *e.g.* by diagonalising the Hessian, that $\widehat{\mathbf{H}}$ becomes singular, yet remains finite when eigenvalues of $\mathbf{H}$ degenerate). The trajectory of the critical point continues smoothly through the top-point, where its "temporal sense" is reversed. This picture of the generic catastrophe captures the fact that there are always pairs of critical points of opposite Hessian signature that "belong together", either because they share a common fate (annihilation) or because they have a common cause (creation). The two members of such a pair could therefore be seen as manifestations of a single "topological particle" if one allows for a non-causal interpretation, in much the same way as one can interpret positrons as instances of electrons upon time-reversal. The analogy with particle physics can be pursued further, as Kalitzin points out, by modeling catastrophes in scale-space as interactions conserving a topological charge [17]. Indeed, charges are operationally well-defined conserved quantities that add up under point interactions at non-Morse critical points, irrespective their degree of degeneracy. This interpretation has the advantage that one can measure charges from spatial surface integrals around the point of interest (by using Stokes' theorem), thus obtaining a "summary" of qualitative image structure in the interior irrespective of whether the enclosed critical points are generic or not. So far, however, Kalitzin's approach has not been refined to the sub-voxel domain, and does not give us a local parametrisation of the critical curve.

The perturbative approach can be extended to higher orders without essential difficulties, yielding a local parametrisation of the critical path of corresponding order. It remains a notorious problem to find the *optimal order* in numerical sense, because it is clear that although the addition of yet another order will *reduce* the formal truncation error due to the smaller Taylor tail discarded, it will at the same time *increment* the amount of intrinsic noise due to the computation of higher order derivatives. It is beyond the scope of this paper to deal with this issue in detail; a point of departure may be Blom's study of noise propagation under simultaneous differentiation and blurring [3]. We restrict our attention to lowest nontrivial order. For Morse critical points this is apparently third order, for top-points this will be seen to require fourth order derivatives.

If one knows the location of the top-point one can find a similar critical curve parametrisation in terms of the parameter τ, starting out from this top-point instead of a Morse critical point. In that case we first have to solve the top-point localisation problem. It is clearly of interest to know the parametrisation *at the top-point*, since this will enable us to identify the two corresponding branches of the Morse critical curves that are glued together precisely at this point. Our next objective will be to find the location of the top-point with sub-voxel precision, as well as geometric properties of the critical curve passing through.

2.4.2 Top-Points

The reason why we must be cautious near top-points is that Eq. (21) breaks down at degeneracies of the Hessian, and is therefore likely to produce unreliable results as soon as we come too close to such a point. A differential invariant [7] that could be used to trigger an alarm[10] is $t_\lambda = \sigma^{2n}\|\mathbf{g}\|^{2n} + \lambda\,\sigma^{4n}\det^2\mathbf{H}$ for any $\lambda > 0$ (exponents have been chosen as such for reasons of homogeneity); in the generic case $t_\lambda(\mathbf{x}_0;t_0) = 0$ iff $(\mathbf{x}_0;t_0)$ is a top-point. "Hot-spots" in scale-space thus correspond to regions where $t_\lambda(\mathbf{x};t)$ becomes smaller than some suitably chosen small parameter times its average value over the scale-space domain (say). In those regions we must study the full system of Eq. (19), including the degeneracy constraint. The additional scale degree of freedom obviously becomes essential, because top-points will typically be located in-between two precomputed levels of scale.

Recall Eq. (16). Let us rewrite the corresponding cofactor matrix, the Cartesian coefficients of

[10] A zero-crossings method for g and $\det\mathbf{H}$ is, however, the preferred choice, as it preserves connectivity.

which are defined by (*cf.* Appendix A)

$$\widetilde{\mathrm{M}}^{\mu\nu} \stackrel{\text{def}}{=} \frac{1}{n!}\,\varepsilon^{\mu\mu_1\ldots\mu_n}\,\varepsilon^{\nu\nu_1\ldots\nu_n}\,\mathrm{M}_{\mu_1\nu_1}\ldots\mathrm{M}_{\mu_n\nu_n}\,, \tag{24}$$

into a similar block form:

$$\widetilde{\mathrm{M}} \stackrel{\text{def}}{=} \begin{bmatrix} \overline{\mathbf{H}} & \overline{\mathbf{w}} \\ \overline{\mathbf{z}}^{\mathrm{T}} & \overline{\mathrm{c}} \end{bmatrix}. \tag{25}$$

By substitution one may verify that the defining equation $\widetilde{\mathrm{M}}\mathrm{M} = \det\mathrm{M}\,\mathbf{I}_{(n+1)\times(n+1)}$ is satisfied iff the coefficients are defined as follows:

$$\overline{\mathbf{H}}^{\mu\nu} \stackrel{\text{def}}{=} \frac{1}{(n-1)!}\,\varepsilon^{\mu\mu_1\ldots\mu_{n-1}}\,\varepsilon^{\nu\nu_1\ldots\nu_{n-1}}\,\mathbf{H}_{\mu_1\nu_1}\ldots\mathbf{H}_{\mu_{n-2}\nu_{n-2}}\,(\mathrm{c}\,\mathbf{H}_{\mu_{n-1}\nu_{n-1}} - (n-1)\,\mathbf{w}_{\mu_{n-1}}\mathbf{z}_{\nu_{n-1}}) \tag{26}$$

$$\overline{\mathbf{w}}^{\mu} \stackrel{\text{def}}{=} -\frac{1}{(n-1)!}\,\varepsilon^{\mu\mu_1\ldots\mu_{n-1}}\,\varepsilon^{\nu\nu_1\ldots\nu_{n-1}}\,\mathbf{H}_{\mu_1\nu_1}\ldots\mathbf{H}_{\mu_{n-1}\nu_{n-1}}\mathbf{w}_{\nu}\,, \tag{27}$$

$$\overline{\mathbf{z}}^{\mu} \stackrel{\text{def}}{=} -\frac{1}{(n-1)!}\,\varepsilon^{\mu\mu_1\ldots\mu_{n-1}}\,\varepsilon^{\nu\nu_1\ldots\nu_{n-1}}\,\mathbf{H}_{\mu_1\nu_1}\ldots\mathbf{H}_{\mu_{n-1}\nu_{n-1}}\mathbf{z}_{\mu}\,, \tag{28}$$

$$\overline{\mathrm{c}} \stackrel{\text{def}}{=} \frac{1}{n!}\,\varepsilon^{\mu_1\ldots\mu_n}\,\varepsilon^{\nu_1\ldots\nu_n}\,\mathbf{H}_{\mu_1\nu_1}\ldots\mathbf{H}_{\mu_n\nu_n}\,. \tag{29}$$

Note that $\overline{\mathbf{z}} = -\widetilde{\mathbf{H}}\mathbf{z}$, $\overline{\mathbf{w}} = -\widetilde{\mathbf{H}}\mathbf{w}$, and $\overline{\mathrm{c}} = \det\mathbf{H}$. Recalling Eq. (23) one observes that $(\overline{\mathbf{w}};\overline{\mathrm{c}}) = (\mathbf{v}';\mathrm{c}')$. Also,

$$\det\mathrm{M} = \frac{1}{n!}\,\varepsilon^{\mu_1\ldots\mu_n}\,\varepsilon^{\nu_1\ldots\nu_n}\,\mathbf{H}_{\mu_1\nu_1}\ldots\mathbf{H}_{\mu_{n-1}\nu_{n-1}}\,(\mathrm{c}\,\mathbf{H}_{\mu_n\nu_n} - n\,\mathbf{w}_{\mu_n}\mathbf{z}_{\nu_n})\,, \tag{30}$$

or, in coordinate-free notation, $\det\mathrm{M} = \mathrm{c}\det\mathbf{H} - \mathrm{tr}\,(\widetilde{\mathbf{H}}\mathbf{w}\mathbf{z}^{\mathrm{T}})$. At the location of a critical point this is proportional to the scale-space scalar product of the critical point's scale-space velocity and the scale-space normal of the Hessian zero-crossing (recall Eqs. (14–15) and Eq. (23) and the remark above):

$$\det\mathrm{M} = \mathbf{z}^{\mathrm{T}}\,\overline{\mathbf{w}} + \mathrm{c}\,\overline{\mathrm{c}} = \mathbf{w}^{\mathrm{T}}\,\overline{\mathbf{z}} + \mathrm{c}\,\overline{\mathrm{c}}\,. \tag{31}$$

Result 3 (Transversality Hessian Zero-Crossing/Critical Curve) *At a top-point the critical path intersects the Hessian zero-crossing transversally.*

This readily follows by inspection of the tangent hyperplane to the Hessian zero-crossing,

$$\mathbf{z}^{\mathrm{T}}\mathbf{x} + \mathrm{c}\,t = 0\,, \tag{32}$$

and the critical curve's tangent vector, Eq. (23). The cosine of the angle of intersection follows from Eq. (31), which is nonzero in the generic case; genericity implies transversality.

With the established results it is now possible to invert the linear system of Eq. (19); just note that

$$\mathrm{M}^{\text{inv}} = \frac{1}{\det\mathrm{M}}\widetilde{\mathrm{M}}\,, \tag{33}$$

so that

$$\begin{bmatrix} \mathbf{x} \\ t \end{bmatrix} = -\frac{1}{\det\mathrm{M}}\begin{bmatrix} \overline{\mathbf{H}}\mathbf{g} + \overline{\mathbf{w}}\overline{\mathrm{c}} \\ \overline{\mathbf{z}}^{\mathrm{T}}\mathbf{g} + \overline{\mathrm{c}}\overline{\mathrm{c}} \end{bmatrix}. \tag{34}$$

The expression is valid in any coordinate system as required. Note that the sign of $\det\mathrm{M}$ subdivides the image domain into regions to which all generic catastrophes are confined. In fact, the following lemma holds.

Lemma 1 (Segregation of Creations and Annihilations) $\det \mathbf{M} < 0$ *at annihilations,* $\det \mathbf{M} > 0$ *at creations.*

One way to see this is to note that it holds for the canonical forms $f^{\mathrm{A}}(\mathbf{x};t)$ and $f^{\mathrm{C}}(\mathbf{x};t)$ of Definition 2. If we now transform these under an arbitrary coordinate transformation that leaves the diffusion equation invariant, it is easily verified that the sign of $\det \mathbf{M}$ is preserved. An alternative proof based on geometric reasoning is given below.

Proof 1 (Lemma 1) First consider an annihilation event, and recall Eq. (14), and the geometric interpretation of Eqs. (27) and (29) as the scale-space velocity given by Eq. (23). As the topological particle with positive charge (*i.e.* the Morse-critical point with $\det \mathbf{H} > 0$) moves towards the catastrophe (towards increasing scale), the magnitude of $\det \mathbf{H}$ must necessarily decrease. By the same token, as the anti-particle ($\det \mathbf{H} < 0$) moves away from the catastrophe (towards decreasing scale), the magnitude of $\det \mathbf{H}$ must decrease as well. But recall that at the catastrophe $\det \mathbf{M} = \mathbf{z}^{\mathrm{T}} \overline{\mathbf{w}}$ is just the directional derivative of $\det \mathbf{H}$ in the direction of motion as indicated. Therefore $\det \mathbf{M} < 0$.

Next consider a creation event. The positive particle now escapes the singularity in the positive scale direction, whereas the negative particle approaches it in the negative scale direction, so that along the prescribed path $\det \mathbf{H}$ must necessarily increase. In other words, $\det \mathbf{M} > 0$ at the catastrophe. This completes the proof.

The lemma is a special case of the following, more general result, which gives us the curvature of the critical path at the catastrophe.

Result 4 (Curvature of Critical Path at the Catastrophe) *At the location of a generic catastrophe the critical path satisfies*

$$t = \frac{1}{2} \frac{1}{\det \mathbf{M}} \left(\mathbf{z}^{\mathrm{T}} \mathbf{x} \right)^2 + \mathcal{O}(\|\mathbf{x}\|^3, \|\mathbf{x}\| \, t, t^2) \, .$$

The curvature of the critical path at the catastrophe is given by $(\overline{\mathbf{w}}^{\mathrm{T}} \nabla)^2 \, t_{\mathrm{catastrophe}} = \det \mathbf{M}$.

Proof 2 (Result 4) Consider the local 2-jet expansion at the location of a generic catastrophe:

$$\begin{cases} \nabla \overset{(2)}{L} (\mathbf{x};t) & = & 0 \, , \\ \det \nabla \nabla^{\mathrm{T}} \overset{(2)}{L} (\mathbf{x};t) & = & 0 \, , \end{cases}$$

in which $L_\mu = 0$ and $\| L_{\mu\nu} \| = 0$. From this it follows that along the critical path through the catastrophe

$$\Delta L_\mu t = -L_{\mu\nu} x^\nu - \frac{1}{2} L_{\mu\nu\rho} x^\nu x^\rho + \mathcal{O}(\|\mathbf{x}\|^3, \|\mathbf{x}\| \, t, t^2) \, .$$

Contraction with $\mathbf{z}_\nu \widetilde{L}^{\mu\nu}$, noting that $\widetilde{L}^{\mu\nu} L_{\nu\rho} = 0$ at the catastrophe, and using Eq. (27), yields

$$\mathbf{z}^{\mathrm{T}} \overline{\mathbf{w}} \, t_{\mathrm{catastrophe}} = \frac{1}{2} \left(\mathbf{z}^{\mathrm{T}} \mathbf{x} \right)^2 \, .$$

Note that the first order directional derivative $\overline{\mathbf{w}}^{\mathrm{T}} \nabla t = \mathrm{tr} \, (\widetilde{\mathbf{H}} \mathbf{H}) = 0$ at the catastrophe, so that first order terms disappear. Also recall that $\mathbf{z}^{\mathrm{T}} \overline{\mathbf{w}} = \det \mathbf{M}$ at such a point, so that the first result follows. Straightforward differentiation produces the curvature expression.

2.4.3 Explicit Results from the Covariant Formalism

Having established covariant expressions we have drawn several geometric conclusions that do not follow from the canonical formalism. Here we give a few more examples, using explicit Cartesian coordinates.

Example 1 (Tangent Vector to Critical Curve) At any point on the critical curve—including the top-point—the scale-space tangent vector is proportional to that given by Eq. (23). In 2D Cartesian coordinates we have

$$\begin{bmatrix} \mathbf{v}'_x \\ \mathbf{v}'_y \\ \mathrm{c}' \end{bmatrix} = \begin{bmatrix} -(L_{xxx} + L_{xyy})L_{yy} + (L_{xxy} + L_{yyy})L_{xy} \\ (L_{xxx} + L_{xyy})L_{xy} - (L_{xxy} + L_{yyy})L_{xx} \\ L_{xx}L_{yy} - L_{xy}^2 \end{bmatrix} .$$

Example 2 In 2D the tangent plane to the Hessian zero-crossing in scale-space is given by the following equation in any Cartesian coordinate system:

$$\begin{aligned} &(L_{xxx}L_{yy} + L_{xx}L_{xyy} - 2L_{xy}L_{xxy})\,x + (L_{yyy}L_{xx} + L_{yy}L_{xxy} - 2L_{xy}L_{xyy})\,y + \\ &\quad ((L_{xxyy} + L_{yyyy})L_{xx} + (L_{xxxx} + L_{xxyy})L_{yy} - 2(L_{xxxy} + L_{xyyy})L_{xy})\,t = 0 . \end{aligned}$$

Example 3 (Segregation of Creations and Annihilations) In a full $(2+1)$D scale-space neighbourhood of an annihilation (creation) the following differential invariant always has a negative (positive) value:

$$\begin{aligned} &\det \mathbf{M} = \\ &\quad ([L_{xxyy} + L_{yyyy}]L_{xx} + [L_{xxxx} + L_{xxyy}]L_{yy} - 2[L_{xxxy} + L_{xyyy}]L_{xy})(L_{xx}L_{yy} - L_{xy}^2) + \\ &\quad -\{L_{xx}[L_{xxy} + L_{yyy}][L_{yyy}L_{xx} + L_{yy}L_{xxy} - 2L_{xy}L_{xyy}] + \\ &\quad +L_{yy}[L_{xxx} + L_{xyy}][L_{xxx}L_{yy} + L_{xx}L_{xyy} - 2L_{xy}L_{xxy}] + \\ &\quad -L_{xy}([L_{xxx} + L_{xyy}][L_{yyy}L_{xx} + L_{yy}L_{xxy} - 2L_{xy}L_{xyy}] + \\ &\quad [L_{xxy} + L_{yyy}][L_{xxx}L_{yy} + L_{xx}L_{xyy} - 2L_{xy}L_{xxy}])\} \end{aligned}$$

The expressions are a bit complicated, but nevertheless follow straightforwardly from their condensed covariant counterparts, which at the same time illustrates the power of the covariant formalism.

3 Conclusion and Discussion

We have described the deep structure of a scale-space image in terms of an operational scheme to characterise, detect and localise critical points in scale-space. The characterisation pertains to local geometrical properties of the scale-traces of individual critical points (locations, angles, directions, velocities, accelerations), as well as to topological ones. The latter fall into two categories, local and bilocal properties. The characteristic local property of a critical point is determined by its Hessian signature (Morse i-saddle or top-point), which in turn defines its topological charge. The fact that pairs of critical points of opposite charge can be created or annihilated as resolution decreases determines bilocal connections; such pairs of critical points can be labelled according to their common fate or cause, *i.e.* they can be linked to their corresponding catastrophe (annihilation, respectively creation). This possibility to establish links is probably the most important topological feature provided by the Gaussian scale-space paradigm.

Conceptually a scale-space representation is a continuous model imposed on a discrete set of pixel data. The events of topological interest in this scale-space representation are clearly the top-points, and

the question presents itself whether these discrete events in turn suffice to define a complete and robust discrete representation of the continuous scale-space image (possibly up to a trivial invariance). In the 1D case it has been proven to be possible to reconstruct the initial image data from its scale-space top-points, at least in principle [16], but the problem of robustness and the extension to higher dimensions is still unsolved. The solution to this problem affects multiresolution schemes for applications beyond image segmentation, such as registration, coding, compression, *etc.*

Acknowledgement

James Damon of the University of North Carolina is gratefully acknowledged for his clarifications.

A Determinants and Cofactor Matrices

Definition 3 (Transposed Cofactor Matrix) *Let* $\mathbf{A}$ *be a square* $n \times n$ *matrix with components* $a_{\mu\nu}$*. Then we define the transposed cofactor matrix* $\widetilde{\mathbf{A}}$ *as follows. In order to obtain the matrix entry* $\widetilde{a}^{\mu\nu}$ *skip the* μ*-th column and* ν*-th row of* $\mathbf{A}$*, evaluate the determinant of the resulting submatrix, and multiply by* $(-1)^{\mu+\nu}$ *("checkerboard pattern"). Or, using tensor notation,*

$$\widetilde{\mathbf{A}}^{\mu\nu} \stackrel{\text{def}}{=} \frac{1}{(n-1)!}\, \varepsilon^{\mu\mu_1\ldots\mu_{n-1}}\, \varepsilon^{\nu\nu_1\ldots\nu_{n-1}}\, \mathbf{A}_{\mu_1\nu_1} \ldots \mathbf{A}_{\mu_{n-1}\nu_{n-1}} \,.$$

By construction we have $\mathbf{A}\,\widetilde{\mathbf{A}} = \det \mathbf{A}\, \mathbf{I}$. Note that if the components of $\mathbf{A}$ are indexed by lower indices, then by convention one uses upper indices for those of $\widetilde{\mathbf{A}}$ (*vice versa*). Furthermore, it is important for subsequent considerations to observe that the transposed cofactor matrix is always well-defined, and that its components are homogeneous polynomial combinations of those of the original matrix of degree $n-1$. In the nonsingular case one has $\widetilde{\mathbf{A}} = \det \mathbf{A}\, \mathbf{A}^{\text{inv}}$; transposed cofactor matrix equals inverse matrix times determinant. See *e.g.* Strang [36]. Note that for diagonal matrices determinants and transposed cofactor matrices are straightforwardly computed.

References

[1] V. I. Arnold. *Catastrophe Theory*. Springer-Verlag, Berlin, 1984.

[2] F. Bergholm. Edge focusing. *IEEE Transactions on Pattern Analysis and Machine Intelligence*, 9:726–741, 1987.

[3] J. Blom, B. M. ter Haar Romeny, A. Bel, and J. J. Koenderink. Spatial derivatives and the propagation of noise in Gaussian scale-space. *Journal of Visual Communication and Image Representation*, 4(1):1–13, March 1993.

[4] J. Damon. Local Morse theory for solutions to the heat equation and Gaussian blurring. *Journal of Differential Equations*, 115(2):368–401, January 1995.

[5] L. M. J. Florack. Data, models, and images. Technical Report 96/13, Department of Computer Science, University of Copenhagen, 1996.

[6] L. M. J. Florack. *Image Structure*, volume 10 of *Computational Imaging and Vision Series*. Kluwer Academic Publishers, Dordrecht, The Netherlands, 1997.

[7] L. M. J. Florack, B. M. ter Haar Romeny, J. J. Koenderink, and M. A. Viergever. Cartesian differential invariants in scale-space. *Journal of Mathematical Imaging and Vision*, 3(4):327–348, November 1993.

[8] L. M. J. Florack, B. M. ter Haar Romeny, J. J. Koenderink, and M. A. Viergever. The Gaussian scale-space paradigm and the multiscale local jet. *International Journal of Computer Vision*, 18(1):61–75, April 1996.

[9] L. M. J. Florack, W. J. Niessen, and M. Nielsen. The intrinsic structure of optic flow incorporating measurement duality. *International Journal of Computer Vision*, 27(3):263–286, 1998.

[10] R. Gilmore. *Catastrophe Theory for Scientists and Engineers*. Dover Publications, Inc., New York, 1993. Originally published by John Wiley & Sons, New York, 1981.

[11] L. D. Griffin and A. C. F. Colchester. Superficial and deep structure in linear diffusion scale space: Isophotes, critical points and separatrices. *Image and Vision Computing*, 13(7):543–557, September 1995.

[12] B. M. ter Haar Romeny, L. M. J. Florack, J. J. Koenderink, and M. A. Viergever, editors. *Scale-Space Theory in Computer Vision: Proceedings of the First International Conference, Scale-Space'97, Utrecht, The Netherlands*, volume 1252 of *Lecture Notes in Computer Science*. Springer-Verlag, Berlin, July 1997.

[13] T. Iijima. Basic theory on normalization of a pattern (in case of typical one-dimensional pattern). *Bulletin of Electrical Laboratory*, 26:368–388, 1962. (In Japanese).

[14] P. Johansen. On the classification of toppoints in scale space. *Journal of Mathematical Imaging and Vision*, 4(1):57–67, 1994.

[15] P. Johansen. Local analysis of image scale space. In Sporring et al. [35], chapter 10, pages 139–146.

[16] P. Johansen, S. Skelboe, K. Grue, and J. D. Andersen. Representing signals by their top points in scale-space. In *Proceedings of the 8th International Conference on Pattern Recognition (Paris, France, October 1986)*, pages 215–217. IEEE Computer Society Press, 1986.

[17] S. N. Kalitzin, B. M. ter Haar Romeny, A. H. Salden, P. F. M. Nacken, and M. A. Viergever. Topological numbers and singularities in scalar images. Scale-space evolution properties. To be published in the Journal of Mathematical Imaging and Vision, 1998.

[18] J. J. Koenderink. The structure of images. *Biological Cybernetics*, 50:363–370, 1984.

[19] J. J. Koenderink. The structure of the visual field. In W. Güttinger and G. Dangelmayr, editors, *The Physics of Structure Formation: Theory and Simulation. Proceedings of an International Symposium*, Tübingen, Germany, October 27–November 2 1986. Springer-Verlag.

[20] J. J. Koenderink. A hitherto unnoticed singularity of scale-space. *IEEE Transactions on Pattern Analysis and Machine Intelligence*, 11(11):1222–1224, November 1989.

[21] J. J. Koenderink. *Solid Shape*. MIT Press, Cambridge, 1990.

[22] J. J. Koenderink and A. J. van Doorn. Dynamic shape. *Biological Cybernetics*, 53:383–396, 1986.

[23] J. J. Koenderink and A. J. van Doorn. Representation of local geometry in the visual system. *Biological Cybernetics*, 55:367–375, 1987.

[24] J. J. Koenderink and A. J. van Doorn. Receptive field families. *Biological Cybernetics*, 63:291–298, 1990.

[25] J. J. Koenderink and A. J. van Doorn. The structure of two-dimensional scalar fields with applications to vision. *Biological Cybernetics*, 33:151–158, 1979.

[26] J. J. Koenderink and A. J. van Doorn. Operational significance of receptive field assemblies. *Biological Cybernetics*, 58:163–171, 1988.

[27] T. Lindeberg. On the behaviour in scale-space of local extrema and blobs. In P. Johansen and S. Olsen, editors, *Theory & Applications of Image Analysis*, volume 2 of *Series in Machine Perception and Artificial Intelligence*, pages 38–47. World Scientific, Singapore, 1992. Selected papers from the 7th Scandinavian Conference on Image Analysis.

[28] T. Lindeberg. Scale-space behaviour of local extrema and blobs. *Journal of Mathematical Imaging and Vision*, 1(1):65–99, March 1992.

[29] T. Lindeberg. *Scale-Space Theory in Computer Vision*. The Kluwer International Series in Engineering and Computer Science. Kluwer Academic Publishers, 1994.

[30] T. Lindeberg. Feature detection with automatic scale selection. *International Journal of Computer Vision*, 30(2), 1998. In press.

[31] W. J. Niessen, J. S. Duncan, M. Nielsen, L. M. J. Florack, B. M. ter Haar Romeny, and M. A. Viergever. A multiscale approach to image sequence analysis. *Computer Vision and Image Understanding*, 65(2):259–268, February 1997.

[32] N. Otsu. *Mathematical Studies on Feature Extraction in Pattern Recognition*. PhD thesis, Electrotechnical Laboratory, Ibaraki, Japan, 1981. (In Japanese).

[33] T. Poston and I. N. Stewart. *Catastrophe Theory and its Applications*. Pitman, London, 1978.

[34] L. Schwartz. *Théorie des Distributions*, volume I, II of *Actualités scientifiques et industrielles; 1091,1122*. Publications de l'Institut de Mathématique de l'Université de Strasbourg, Paris, 1950–1951.

[35] J. Sporring, M. Nielsen, L. M. J. Florack, and P. Johansen, editors. *Gaussian Scale-Space Theory*, volume 8 of *Computational Imaging and Vision Series*. Kluwer Academic Publishers, Dordrecht, 1997.

[36] G. Strang. *Linear Algebra and its Applications*. Academic Press, London, second edition, 1980.

[37] R. Thom. *Stabilité Structurelle et Morphogénèse*. Benjamin, Paris, 1972.

[38] R. Thom. *Structural Stability and Morphogenesis (translated by D. H. Fowler)*. Benjamin-Addison Wesley, New York, 1975.

[39] J. Tingleff. Mathematical software for computation of toppoints. Technical Report 90/15, Department of Computer Science, University of Copenhagen, 1990.

[40] K. L. Vincken, A. S. E. Koster, and M. A. Viergever. Probabilistic multiscale image segmentation. *IEEE Transactions on Pattern Analysis and Machine Intelligence*, 19(2):109–120, 1997.

[41] J. A. Weickert, S. Ishikawa, and A. Imiya. On the history of Gaussian scale-space axiomatics. In Sporring et al. [35], chapter 4, pages 45–59.

[42] A. P. Witkin. Scale-space filtering. In *Proceedings of the International Joint Conference on Artificial Intelligence*, pages 1019–1022, Karlsruhe, Germany, 1983.